Electronic Supplementary Information

Enhancement of Photodetection Characteristics of MoS_2 Field Effect Transistors using Surface Treatment with Copper Phthalocyanine

Jinsu Pak,[a] Jingon Jang,[a] Kyungjune Cho,[a] Tae-Young Kim,[a] Jae-Keun Kim,[a] Younggul Song,[a] Woong-Ki Hong,[b] Misook Min,*[a] Hyoyoung Lee,[c] and Takhee Lee*[a]*

[a]Department of Physics and Astronomy, and institute of Applied Physics, Seoul National University, Seoul 08826, Korea
E-mail: minmi0924@gmail.com; tlee@snu.ac.kr
[b]Jeonju Center, Korea Basic Science Institute, Jeonju, Jeollabul-do 54907, Korea
E-mail: wkh27@knsi.re.kr
[c]Center for Integrated Nanostructure Physics, institute for Basic Science (IBS), Department of Energy Science, Department of Chemistry, Sungkyunkwan University, Suwon 16410, Korea

Table of Contents

1. Ti/MoS_2 contact

Figure S1 shows the output characteristic (current versus drain-source voltage; I_{DS}–V_{DS}) plots for MoS_2 FET devices with and without the CuPc layer. These results indicate that the Ti/MoS_2 contacts exhibit ohmic contacts.

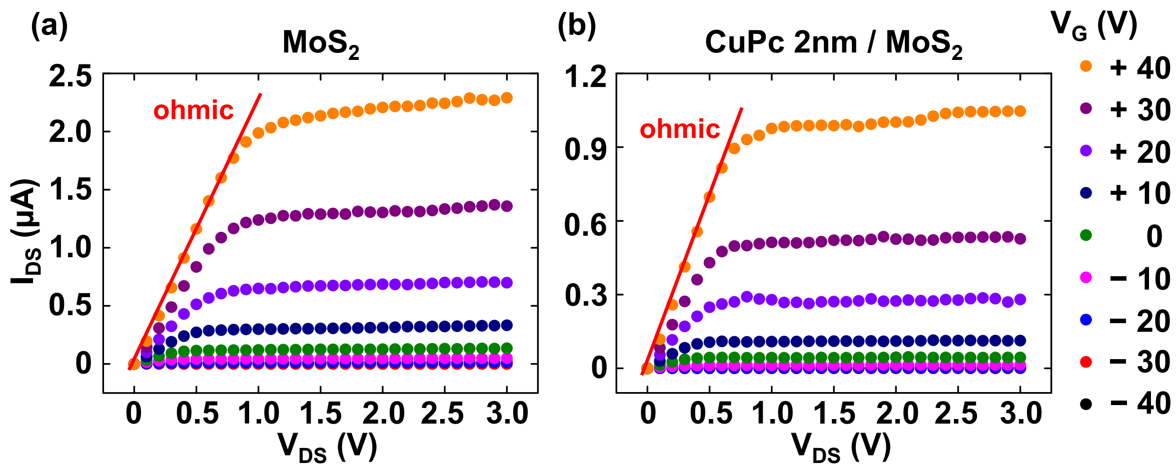

Figure S1. (a) The output characteristics (I_{DS}–V_{DS}) for MoS_2 FETs (a) without and (b) with CuPc layer.

2. Devices Fabrication

Figure S2 shows the device fabrication processes. First, MoS_2 flakes were mechanically exfoliated from a bulk MoS_2 crystal purchased from SPI Supplies. Then, the MoS_2 flakes were transferred on 270 nm-thick SiO_2 on a highly doped p++ Si Wafer (resistivity ~5×10^{-3} Ω/cm) that can be used as a back gate. Proper MoS_2 flakes were located with an optical microscope and the height of selected MoS_2 flakes were measured with atomic force microscope (NX 10 AFM system, Park Systems). To make electrode patterns, we spin-coated methyl methacrylate (9% concentration in ethyl lactate) and PMMA 950K (5% concentration in anisole) at 4000 rpm. After the spin-coating of each layer, the sample was baked at 180 ^{o}C for 90 s on a hot plate. We used an electron beam lithography system (JSM-6510, JEOL) to pattern electrodes. Development of patterns was performed with a MIBK/IPA (1:3) solution for 50 s. Electrodes was made by depositing 30 nm thick Ti with an e-beam evaporator (KVE-2004L, Korea Vacuum Tech). Finally, the copper phthalocyanine (CuPc) was deposited on fabricated MoS_2 field effect transistor (FET) devices by a thermal evaporator (GVTE1000, GV-Tech).

Figure S2. Schematic processes of fabricating MoS_2 FET devices.

3. Raman spectroscopy data

Figure S3a shows the Raman data of a pristine MoS_2 flake before CuPc layer was deposited. We observed that the MoS_2 flake exhibited two Raman characteristic bands at 383 and 405 cm^{-1}, corresponding to the out-of-plane vibration of atoms (A_{1g} mode) and in-plane vibration of atoms (E_{2g} mode) of MoS_2, respectively. Figure S3b shows the Raman data of a CuPc film on MoS_2. In this case, the most intense Raman bands were observed at 1144, 1345, 1454, and 1531 cm^{-1} for pyrrole groups, phthalocyanine, C-N bond, and C-C bond of CuPc, respectively. The Raman peaks represented in Figure S3b suggest that CuPc layer was well deposited on MoS_2 surface.

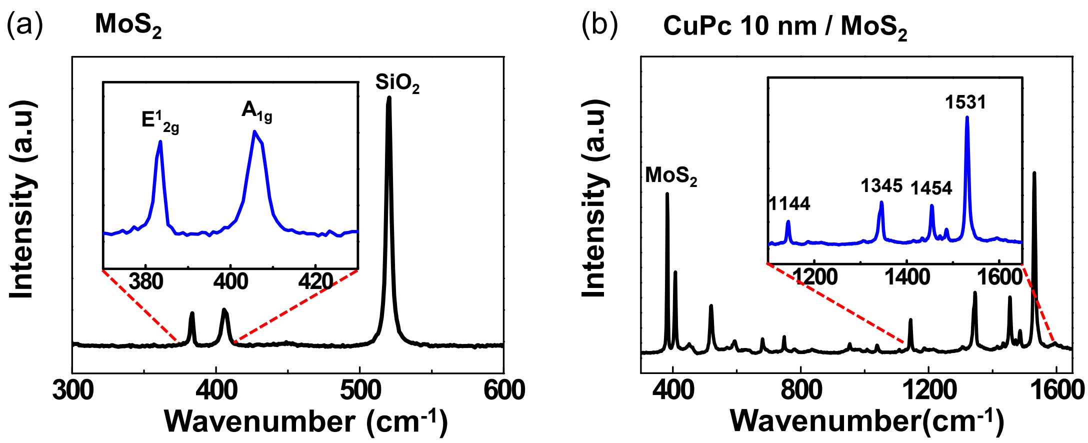

Figure S3. Raman spectroscopy data of (a) pristine MoS_2 and (b) $CuPc/MoS_2$.

4. X-ray photoelectron spectroscopy data

The X-ray photoelectron spectroscopy (XPS) scans on a MoS_2 flake confirmed the chemical bonding states of the Mo and S. The Mo 3d showed two peaks at 229.64 and 232.84 eV, attributed to the Mo $3d_{5/2}$ and Mo $3d_{3/2}$, respectively, in Figure S4a. The S 2p showed two peaks at 163.74 and 162.54 eV, corresponding to the S $2p_{1/2}$ and S $2p_{3/2}$, respectively, in Figure S4b. When the CuPc layer was deposited on MoS_2, the Mo 3d two peaks shifted from 229.64 to 229.04 and from 232.84 to 232.14 eV, attributed to the Mo $3d_{5/2}$ and Mo $3d_{3/2}$, respectively. The S 2p two peaks also shifted from 162.54 to 162.01 and from 163.74 to 163.26 eV, corresponding to the S $2p_{3/2}$ and S $2p_{1/2}$, respectively. In addition, the peaks of Mo and S in the CuPc/MoS_2 show a shift toward lower binding energies compared to those of the pristine MoS_2 flake. This shift is attributed to lowering of the Fermi level upon the p-doping.[S1]

The CuPc-covered MoS_2 flakes showed the element peaks of only Cu, N and C in the XPS spectra. The Cu 2p spectra had two peaks at 934.8 and 954.5 eV, attributed to the Cu $2p_{1/2}$ and Cu $2p_{3/2}$, respectively, in Figure S4c. For the N 1s spectrum, the main peak appeared at 398.8 and a shoulder peak emerged at 400.4 eV (C−N=C bond), shown in Figure S4d. The C 1s showed two peaks at 284.5 and 285.7 eV, corresponding to the C−C bond and C−N bond, respectively, in Figure S4e.

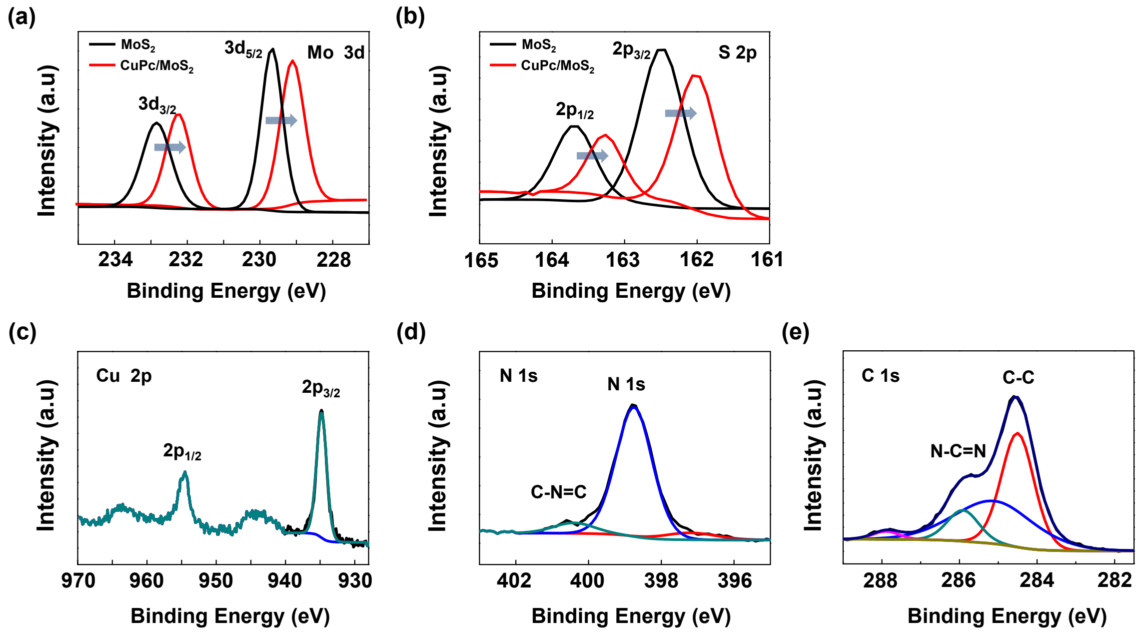

Figure S4. XPS data of MoS_2 and CuPc films.

5. CuPc layer thickness by AFM

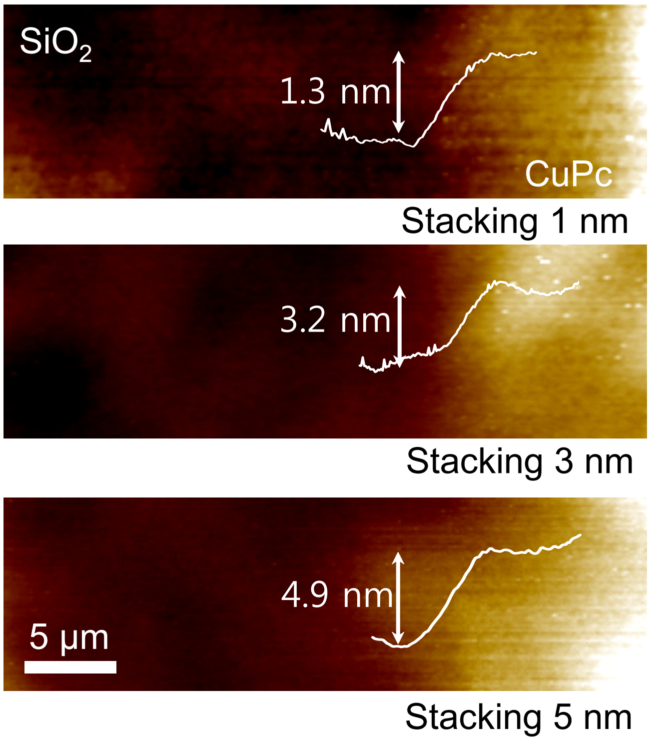

Figure S5. AFM images of CuPc layers deposited by thermal evaporator system.

6. CuPc/MoS_2 hybrid FETs with CuPc layers of 5, 10, 20, and 30 nm thickness

Figures S6a and S6b show the transfer and output characteristics of the CuPc/MoS_2 hybrid FET devices with different CuPc thickness (5, 10, 20, and 30 nm). Consistent with the results in Figure 2 of the main manuscript, the channel current decreased at positive gate voltage and the threshold voltage shifted to the positive gate voltage direction. Figure S6c summarizes the threshold voltage and electron carrier concentration estimated at V_G = 20 V and V_{DS} = 0.1 V for these CuPc/MoS_2 hybrid FET devices.

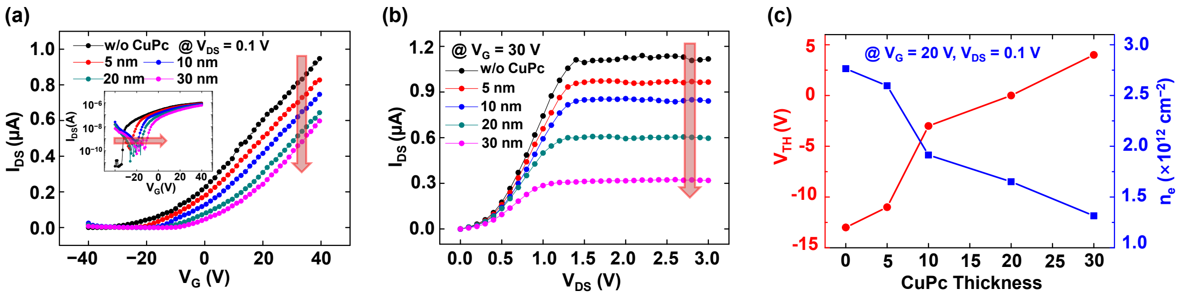

Figure S6. (a) I_{DS}–V_G curves and (b) I_{DS}–V_{DS} curves of CuPc/MoS_2 hybrid FET devices with different CuPc thickness (5, 10, 20, and 30 nm). (c) Threshold voltage and electron carrier concentration for the CuPc/MoS_2 hybrid FET devices.

7. The electron mobility versus the CuPc thickness

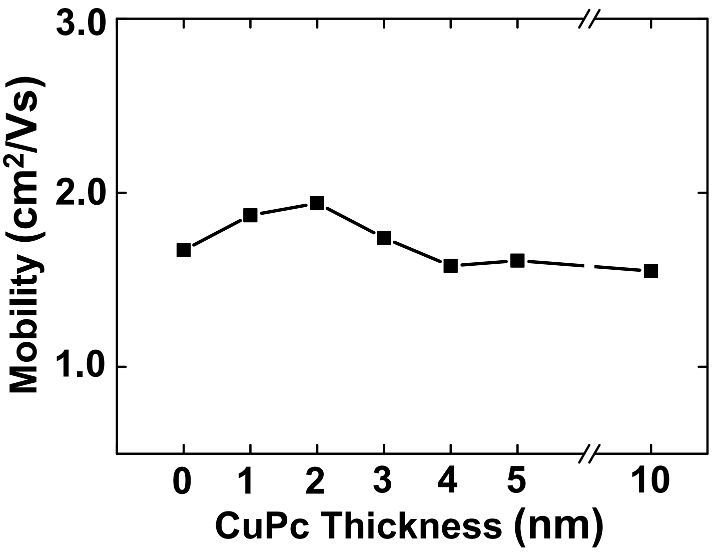

Figure S7**.** The electron mobility as a function of the CuPc thickness.

8. Electrical and photoresponsive properties of CuPc FETs

Figure S8a illustrates the cross-sectional schematic of CuPc-alone FET (i.e., CuPc FET without MoS_2) under light illumination. Figure S8b shows the transfer curves of CuPc FETs with different CuPc layer thickness (3, 5, and 10 nm). The channel current of CuPc FETs increased as the increasing CuPc layer thickness. Inset plot in Figure S8b indicates the channel could not formed when we stacked CuPc layer of 1 nm thickness. This is because 1 nm-thick CuPc was not formed as a uniform film across the source and drain electrodes. Figure S8c exhibits the photoresponsive chracteristics of CuPc FETs under 520 nm light illumination. This data means that the hole carrier density of CuPc increase with the thickness of CuPc.

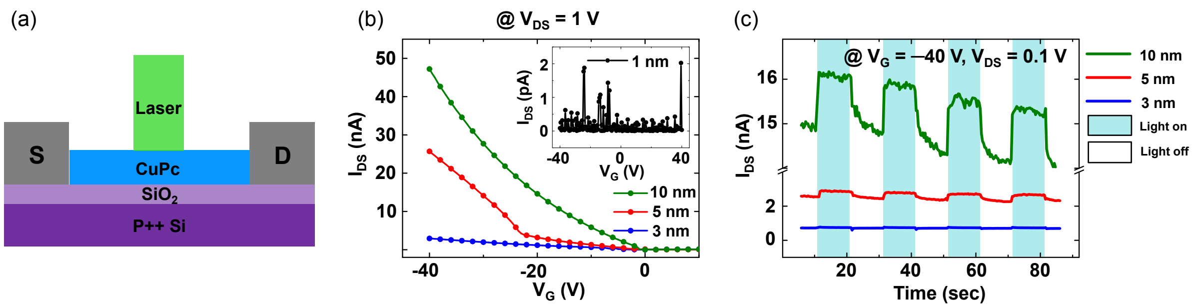

Figure S8. (a) The schematic of a CuPc FET under light illumination (520 nm). (b) I_{DS}–V_G curves of CuPc FETs with different CuPc layer thickness (3, 5 and 10 nm) measured at V_{DS} = 1 V. (c) Photoresponsive data of CuPc FETs measured at V_G = −40 V and V_{DS} = 0.1 V under light on and off.

9. Gate voltage dependence of the phtocurrent and the photoresponsivity

Figure S9 shows the gate-voltage dependence of the photocurrent and the photoresponsivity. The photocurrent and photoresponsivity were enhanced with positively increasing the gate voltage. The application of positive gate voltage leads to increase electron carrier density in the MoS_2 channel layer, but it decrease the hole density in the CuPc layer, which results in the reduction of charge recombination at the interface between MoS_2 and CuPc layers. Interestingly, for the MoS_2 device with the 2 nm-thick CuPc layer, the photocurrent and photoresponsivity were larger than those of the MoS_2 device without the CuPc layer, indicating the photo-generated electrons in the CuPc layer assist enhancement of the photoresponse properties of MoS_2 device.

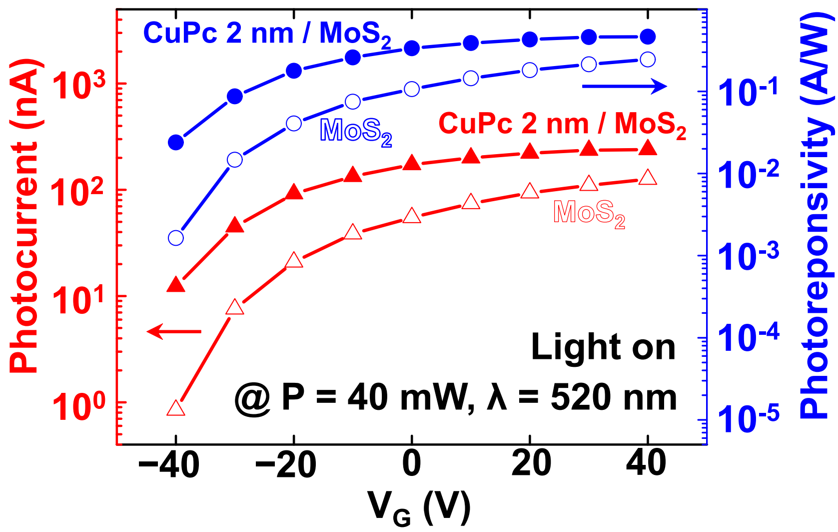

Figure S9. Gate voltage dependence of the photocurrent and the photoresponsivity.

Reference

S1. S. Joonki, P. Tae-Eon, L. Der-Yuh, F. Deyi, P. Joonsuk, J. Hee Joon, C. Yabin, K. Changhyun, J. Chaun, S. Yinghui, S. Robert, C. Joonyeon, T. Sefaattin, W. Junqiao, *Nano Lett.* 2014, **14**, 6976.